Original Article

Synthesis of TiO₂ nanogel composite for highly efficient self-healing epoxy coating

Erfan Rezvani Ghomi [a,b], Saied Nouri Khorasani [a,*], Mohammad Sadegh Koochaki [a,g], Mohammad Dinari [c], Shahla Ataei [a], Mohammad Hossein Enayati [d], Oisik Das [e,*], Rasoul Esmaeely Neisiany [f,*]

[a] Department of Chemical Engineering, Isfahan University of Technology, Isfahan 84156-83111, Iran
[b] Center for Nanotechnology and Sustainability, Department of Mechanical Engineering, National University of Singapore, Singapore 117581, Singapore
[c] Department of Chemistry, Isfahan University of Technology, Isfahan 84156-83111, Iran
[d] Department of Materials Engineering, Isfahan University of Technology, Isfahan 84156-83111, Iran
[e] Structural and Fire Engineering Division, Department of Civil, Environmental and Natural Resources Engineering, Luleå University of Technology, 97187 Luleå, Sweden
[f] Department of Materials and Polymer Engineering, Faculty of Engineering, Hakim Sabzevari University, Sabzevar 9617976487, Iran
[g] Research and Development Department, Alvan Paint & Resin Production Co., Tehran, 13991-53611, Iran

HIGHLIGHTS

- A highly efficient self-healing coating was developed.
- Nanogel composite was synthesized via the in-situ emulsion polymerization method.
- The various amount of nanogel composite were incorporated into the epoxy resin.

GRAPHICAL ABSTRACT
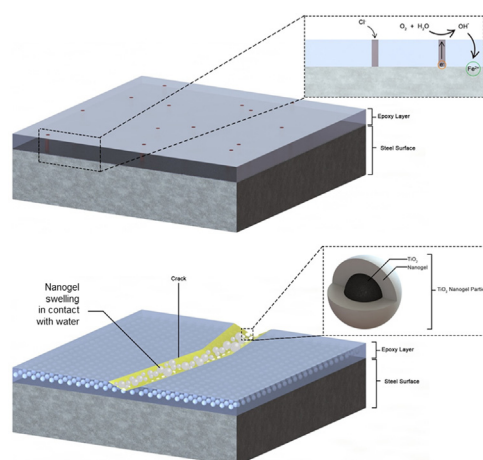
ABSTRACT

Introduction: Organic coatings are the most effective and facile methods of protecting steel against corrosion, which shields it from direct contact with oxygen and moisture. However, they are inherently defective and susceptible to damage, which allows the penetration of the corrosive media into the underlying substrates. Self-healing coatings were developed to address this shortcoming.
Objective: The current research aims to develop a coating with superior self-healing ability via embedment of titanium dioxide (TiO₂) nanogel composite (NC) in a commercial epoxy.
Methods: The TiO₂ NC was prepared by efficient dispersion of TiO₂ nanoparticles in copolymer gel of acrylamide (AAm) and 2-acrylamido-2-methyl propane sulfonic acid (AMPS) with the help of 3-(trimethoxysilyl) propyl methacrylate (MPS). The chemical structure, morphology, and thermal properties of the modified and functionalized nanoparticles were assessed by infrared spectroscopy, electron microscopy, X-ray diffraction, and thermogravimetric analysis, respectively. In addition, TiO₂

Peer review under responsibility of Cairo University.

* Corresponding authors.
    E-mail addresses: saied@iut.ac.ir (S. Nouri Khorasani), oisik.das@ltu.se (O. Das), r.esmaeely@hsu.ac.ir (R. Esmaeely Neisiany).

nanoparticles, nano-TiO$_2$ functionalized monomer (NTFM), and NTFM/AAm/AMPS in different weight percentages were incorporated into epoxy resin to prepare a self-healing coating.

Results: The results confirmed the successful fabrication of the NC. In addition, the incorporation of 1 wt% NTFM/AAm/AMPS led to homogenous dispersion, enhanced anti-corrosive and self-healing performance with the healing efficiencies of 100% and 98%, which were determined by electrochemical impedance spectroscopy (EIS) and potentiodynamic polarization methods, respectively.

Conclusion: The prepared NC was sensitive towards salt concentration, pH, which aids the quick reaction of the TiO$_2$ NC to corrosive ions, once the cracks occur. In addition, this is a unique feature compared to the other self-healing mechanisms, especially, the encapsulation of healing agents, which can be effective as long as the healing agent is present.

Introduction

Metallic alloys, particularly steel, are among the best candidates for use in a wide range of structures. However, steel structures are vulnerable to corrosion and erosion, which cause substantial direct and indirect losses [1,2]. Based on the World Corrosion Organization (WCO) reports, the direct annual corrosion loss is 1.3 to 1.4 trillion euros or 1.3 to 3.5 percent of the gross national product of all countries. Experts believe that such huge economical losses can be recovered up to 25 % by using existing technologies to limit corrosion [3]. Corrosion cannot be completely eliminated; hence, corrosion control methods have been focused on reducing its rate or changing the corrosion mechanism. These methods include cathodic protection, protective coatings, using corrosion inhibitors, or a combination of the aforementioned methods [4-7].

Protective coatings are the most effective and facile methods of protecting steel against corrosion, which shields it from direct contact with oxygen and moisture [8,9]. Organic coatings, especially epoxy resins, are widely used for various metallic structures due to their high chemical stability, superior tensile strength, good bending strength, high thermal resistance, excellent electrical properties, and corrosion-resistant properties. Organic coatings are able to enhance corrosion resistance as well as the durability of metallic structures [10]. However, epoxy resins are inherently defective. The evaporation of solvents during the curing process reduces the resistance of the organic coatings and allows the penetration of corrosive media into the underlying substrates [11]. The aforementioned defects reduce the anti-corrosion performance of the coatings and also lessen the adhesion between the coating and the substrate, resulting in rust, formation of blisters, and ultimately the failure of the coating and the steel substrate [12].

Once corrosion occurs, the organic coating itself is unable to cease the propagation of defective zones and protect the substrate. Self-healing coatings showed the potential to ameliorate this crucial problem of organic coatings by repairing the coating through various approaches [13,14]. Currently, new approaches for self-healing have been utilized including the healing agent's release, reversible bonding, and nanoparticles [15-18]. Among the various approaches, the fabrication of metal oxide NCs has presented a great improvement in corrosion resistance and self-healing performance with the possibility for repeated self-healings [19]. Other approaches, such as the encapsulation of the healing agent, show the ability for one-time self-healing. Nanoparticles can fill the microcracks existing in epoxy coatings due to the evaporation of the solvents and hardeners, and consequently, reduce the susceptible zones in the coatings. However, agglomeration of the nanoparticles is inevitable in such conditions, and avoiding it is possible when dispersed homogenously. Hence, the surface of nanoparticles can be modified by grafting to smart gels. Recently, cerium dioxide, silica, magnetite, zirconia, titanium dioxide, graphene oxide, alumina, talc nanoparticles have been used to produce self-healing epoxy coatings [20-30]. Among them, TiO$_2$ is

well-investigated and proved to be effective in the preparation of self-healing and anti-corrosion coatings [27,28,31-33]. It was verified that the smart flexible polymeric layer on the surface of the nanoparticles enhances their dispersion in an epoxy-based matrix, acting as a self-healing coating [33]. Furthermore, the employed polymeric gels showed a 'smart' behavior in contact with water and corrosive components, providing a segmental motion to heal the damaged areas. Although the approach showed a promising performance, there is a gap in the research about the quantitative assessment of the corrosion and self-healing efficiency. There are mostly feasibility studies on this approach and they have been evaluated by qualitative assessment [34,35].

In light of the aforementioned, the current study aims to synthesize TiO$_2$ NC with better dispersibility in an epoxy matrix to enhance the corrosion resistance and self-healing performance of damaged conventional coatings. Thus, neat TiO$_2$ nanoparticles were firstly functionalized by 3-(trimethoxysilyl) propyl methacrylate (MPS) to prepare nano-TiO$_2$ with a vinyl group on their surfaces. The nano-TiO$_2$ functionalized monomers (NTFM) were then modified with copolymeric smart NC of 2-acrylamido-2-methyl propane sulfonic acid (AMPS) and acrylamide (AAm). The AAm-co-AMPS gel was assumed to be sensitive towards salt concentration, pH, which aids the quick reaction of the TiO$_2$ NC to corrosive ions, once the cracks occur.

Experimental

Materials

TiO$_2$ nanopowder (80% anatase and 20% rutile) was obtained from Neutrino Co. with a mean particle size of 20 nm and was used as a precursor to obtain the NCs. AAm monomer, sodium dodecyl sulfate (SDS), and ethanol were purchased from Merck Chemical Co. (Germany). The other monomer, AMPS, was provided by Sigma-Aldrich (USA) along with MPS. In addition, ammonium persulfate (APS) and *N,N,N',N'*-tetramethylethylenediamine (TEMED) were both obtained from Merck chemical Co. (Germany) and used to initiate and accelerate the polymerization, respectively. The hydrochloric acid (HCl) 37% and Sodium hydroxide (NaOH) were purchased from Merck Chemical Co. and used to adjust the pH during the synthesis process. The EPON^{TM} 828 epoxy resin, having the viscosity of 11–15 Pa.s, was diluted using the 1,6 hexanediol diglycidyl ether (ED 180, as reactive diluent), and was cured using Merginamide A280, as a hardener, and were all provided by Hobum Oleochemicals and was used according to our previous research [33] as a commercial coating. Ethanol was used as a solvent without further purification. Deionized water was utilized for all experimental procedures.

Synthesis of TiO$_2$ NC

Firstly, 500 mg TiO$_2$ nanoparticles were introduced to ethanol/ water solution with a volume ratio of 4:1, and then sonicated for

one hour using an ultra-sonication at 400 W. Secondly, MPS (1.568 g, 0.006 mol) was combined with ethanol (10 mL), stirred for one hour, and then was fed to the TiO_2 solution. Thirdly, the prepared mixture was reflux-heated for 8 h at 70 °C. Finally, the resulting product was centrifuged after cooling to room temperature, washed by ethanol, and kept to dry in a vacuum oven at 50 °C overnight to obtain the NTFM. [36].

The NTFM/AAm/AMPS NC was synthesized via free radical copolymerization. Initially, the flask was charged with SDS (0.045 g, 1 wt%) and NTFM (0.2 g) in deionized water and sonicated for 1 h. Next, AAm (1.136 g) and AMPS (3.32 g) were slowly added to the mixture. To neutralize the AMPS monomer, the NaOH solution was used and the pH of the solution in the reactor was adjusted to 8.5 ± 0.5 [37]. The initiator system containing TEMED (30 μL) and APS (1.5 wt%) were dissolved in 10 mL deionized water and dropped into the reaction mixture for 30 min. The reactor was placed in an oil bath to adjust the temperature in a precise manner. The polymerization process took place at 60 °C for 5 h. Afterward, the reactor and mixture were cooled to room temperature, and a highly viscous solution was obtained. Subsequently, acetone was used to precipitate the product, having a white and cotton-like shape. The obtained precipitation was then dried in an oven at 40 °C for 10 h until a constant weight was obtained. The dried sample was then ground and sieved through mesh number 200. Fig. 1 schematically shows the proposed chemical reactions during the functionalizing of TiO_2 nanoparticles and the preparation of TiO_2 NC [38].

Preparation of coating

Before coating with the epoxy, the ST 37 carbon steel panels ($150 \times 100 \times 1$ mm^3) were firstly polished using sandpapers and then degreased with acetone to prepare their surface and remove any rust or dirt.

The EPON 828 epoxy resin was diluted with ED180 in a weight ratio of diluent/epoxy: 1:3. The TiO_2 NCs were then dispersed in the diluted epoxy resin by employing a mechanical mixer for 5 min, working at 200 rpm, at three different contents of 1, 2, and 4 wt% with respect to the total weight of the epoxy resin and its curing agent. All the mixtures containing NTFM/AAm/AMPS, NTFM, and TiO_2 nanoparticles, and also the control sample (neat epoxy resin named as CTRL) were mixed with the Merginamide A280 hardener in a weight proportion of 100:58 (epoxy: hardener) just before their application on the steel plates. The coding of the prepared coatings and the amount of incorporated fillers are summarized in Table 1. The amount of TiO_2 nanoparticles and NTFM incorporated into the epoxy matrix has been calculated from the thermogravimetric analysis (TGA) results. The above-mentioned mixtures were coated on the prepared panels using a universal film applicator (ZEHTNER ZAU 2000.80). To complete the curing process of the coatings, they were kept for 168 h at room temperature (25 ± 2 °C).

Characterization of NC synthesis

The Fourier transform infrared (FTIR) spectra of the pristine TiO_2 nanoparticles, MPS, NTFM, and NTFM/AAm/AMPS samples were recorded with a Ray-Leigh WQF-510A FTIR spectrometer in the range of 4000–400 cm^{-1} using KBr pellets to confirm the successful surface modification and grafting process.

The X-ray diffraction (XRD) spectra were obtained with an ASENWARE (AW-XDM300) diffractometer using CuKα radiation produced at 40 kV and 30 mA in the range of 5-80°, to reveal the formation of copolymer gel on the NTFM particles.

The NC morphology and distribution of NTFM in NTFM/AAm/AMPS gel were investigated using Field emission scanning electron microscopy (FESEM) (Quanta 450 FEG) and Energy-dispersive X-ray spectroscopy (EDS) (Octane Elite EDS). Furthermore, the EDS investigation was employed to determine the elements in the samples and their distribution map has been provided to observe the dispersion of NTFM in the NTFM/AAm/AMPS matrix.

The thermal stability and grafting efficiency of NTFM and TiO_2 NC were determined by TGA (Mettler TGA/SDTA 851e, USA). The samples were analyzed at a temperature range of 25 to 700 °C with a heating rate of 10 °C/min in an Argon atmosphere. The MPS-grafting efficiency percentage ($\%E_g$) was determined as the mass of grafted MPS (m_s) divided by the mass of TiO_2 nanoparticles (m_{TiO2}) at 700 °C according to the following Eq. (1) [36]:

$$\%E_g = m_s/m_{TiO2} \times 100 \tag{1}$$

The swelling ability of the synthesized NC was measured in distilled water. The swelling ratio (SR) of the TiO_2 NC was measured via Eq. (2) [39]:

$$SR=(W_{wet}-W_{dry})/W_{dry} \tag{2}$$

SR is reported based on the gram of the absorbed water ($W_{wet}-W_{dry}$) to the gram of dry NC (W_{dry}).

Assessment of physicomechanical properties

The Gloss test (ISO 2813–2014, SH260C Glossmeter, Sheen Instruments UK) was conducted to study the visual properties of prepared samples as well as to provide an estimate about proper dispersion or agglomeration of particles in the coating matrix. Each sample was tested at a 20° angle three times and the average values were reported.

The prepared coatings' adhesion strength was evaluated by the pull-off adhesion test (ASTM D4541, Positest AT-M, DeFelsko, USA) to study the effect of incorporating TiO2 nanoparticles NTFM, and NTFM/AAm/AMPS into the epoxy matrix.

The total elongation of the prepared coatings was measured via mandrel bend tests using a Conical Mandrel Bend Tester (SH 801, Sheen Instruments, UK). The test was conducted according to ASTM D 522 – Test Method A, and the percentage of the total elongation was reported.

Self-healing evaluation

The corrosion performance of the aforementioned coatings was studied using electrochemical techniques. The EIS and potentiodynamic polarization tests were conducted by a PARSTAT 2273 electrochemical workstation system in a lab-made three-electrode system to assess the self-healing performance of the prepared coatings. A Platinum rod, Ag/AgCl, and the epoxy coatings have been employed as the counter electrode, reference electrode, and working electrode, respectively. All the electrochemical tests were performed in a 3.5 wt% NaCl solution as the selected electrolyte. The coated samples were scratched by a razor blade to make an X shape crack in the coatings' matrix, deep enough to expose the substrate metal. Measurements were conducted on the scratched coatings with an electrolyte exposed area of 0.785 cm^2 after immersion in 3.5 wt% NaCl for 18 days. The scratch dimensions and the electrochemical cell assembly have been reported in detail in our previous work [40]. The EIS tests were carried out at open circuit potential (OCP) within the frequency sweep range of 10^5 to 10^{-2} Hz using a 10 mV amplitude sinusoidal voltage. In order to reach minimal noise interference, all the measurements were conducted in a faraday cage. The potentiodynamic polarization scans were also carried out on the samples at a scan rate of 1 mV/s and the Tafel extrapolation method was employed to evaluate their polarization parameters.
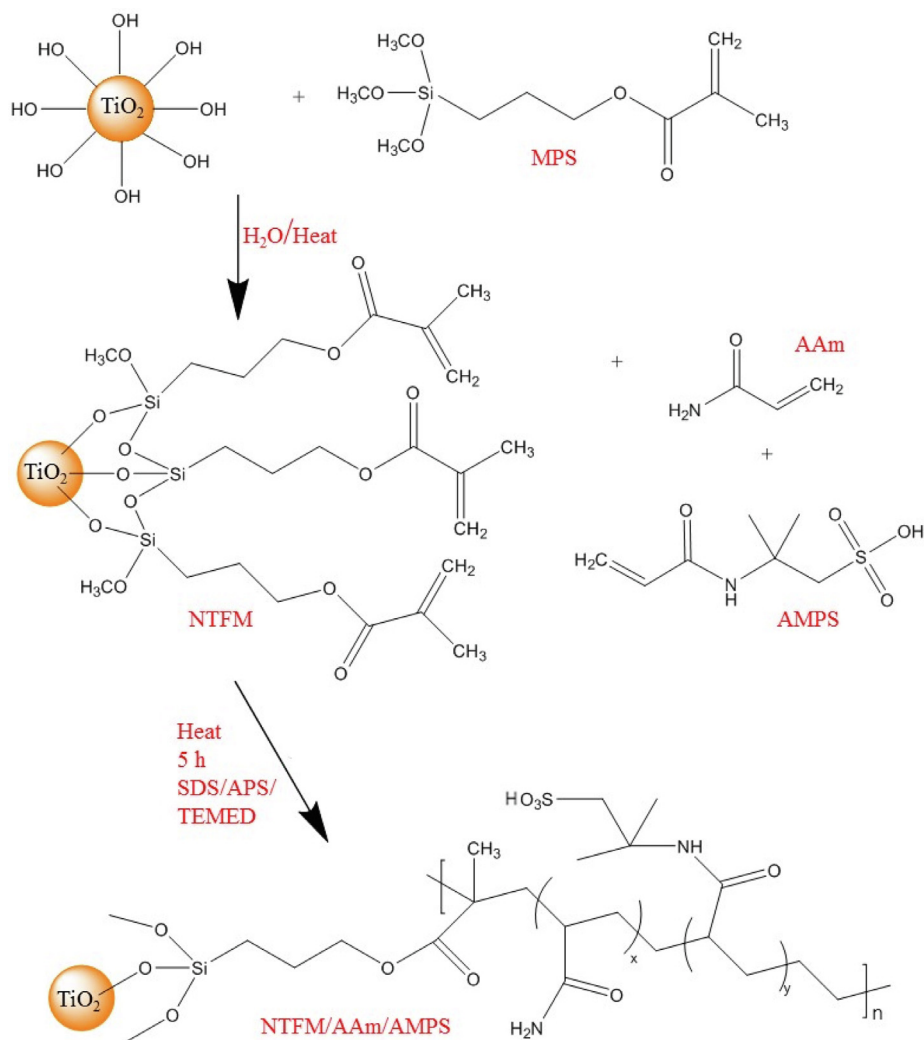
E. Rezvani Ghomi, S. Nouri Khorasani, Mohammad Sadegh Koochaki et al.

Journal of Advanced Research 43 (2023) 137–146

Fig. 1. The proposed schematic illustration of the chemical reactions through the TiO₂ surface modification and TiO₂ NC preparation.

Table 1
The coding of the coated samples.

Sample code	Epoxy resin filled with
CTRL	–
C-T1	1 wt% of neat nano-TiO₂
C-T2	2 wt% of neat nano-TiO₂
C-T4	4 wt% of neat nano-TiO₂
C-NTFM1	1 wt% of NTFM
C-NTFM2	2 wt% of NTFM
C-NTFM4	4 wt% of NTFM
C- NTFM/AAm/AMPS1	1 wt% of NTFM/AAm/AMPS
C-NTFM/AAm/AMPS2	2 wt% of NTFM/AAm/AMPS
C-NTFM/AAm/AMPS4	4 wt% of NTFM/AAm/AMPS

Results and discussion

Evaluations of TiO₂ NC synthesis

It is challenging to prepare spherical TiO₂ nanoparticles and to this end, their surface should be modified to improve their properties before applying to environmental technology. For this reason, firstly, the surface of TiO₂ nanoparticles has been functionalized with MPS to include the vinyl group in the structure of the nanoparticles. The functionalization occurs through hydroxyl groups on the TiO₂ nanoparticles' surface by a condensation reaction, which produces water as the by-product. Next, the function-

alized nanoparticles were polymerized with AAm and AMPS monomers. Fig. 2a shows the FTIR spectra of the samples. Considering the FTIR spectrum of the neat TiO₂ nanoparticles, only hydroxyl groups can be observed on their surface at ca. 3100–3500 and 1640 cm⁻¹. The reactive silanetriol is formed by the hydrolyzation of the methoxy groups in the MPS, which quickly reacts with the hydroxyl groups on the surfaces of the TiO₂ nanoparticles to form a covalent bond [27,32]. The C = C bonds on the NTFM, which appeared at 1635 cm⁻¹, are able to polymerize with acrylamide monomers, leading to a polymeric shell surrounding the TiO₂ core [41]. Regarding the NTFM/AAm/AMPS FTIR spectrum, new peaks appeared that confirm the presence of both AAm and AMPS in the final product [38]. The obtained results verified the success of the chemical grafting of the AAm/AMPS copolymer to the surface of modified TiO₂. As shown in Fig. 2b, the XRD spectra indicated the diffraction peaks of the TiO₂ nanoparticles, NTFM, and NTFM/AAm/AMPS. Based on the diffractograms, the presence of TiO₂ in the NC can be deduced. The strong diffraction peaks at 2θ = 25.3, 37.9, 48.3, 54°, for TiO₂ nanoparticles were assigned to the anatase TiO₂ phase [27]. According to Fig. 2b, surface modification by MPS insignificantly affected the crystalline phase of TiO₂ nanoparticles [42]. The broad amorphous peak at 2θ = 10–30∘ is a sign of copolymer synthesis. Comparing the XRD spectra of the NTFM and TiO₂ NC confirms a decrease in the peak intensity at 25.3∘ of TiO₂ nanocomposite, which can be attributed to the
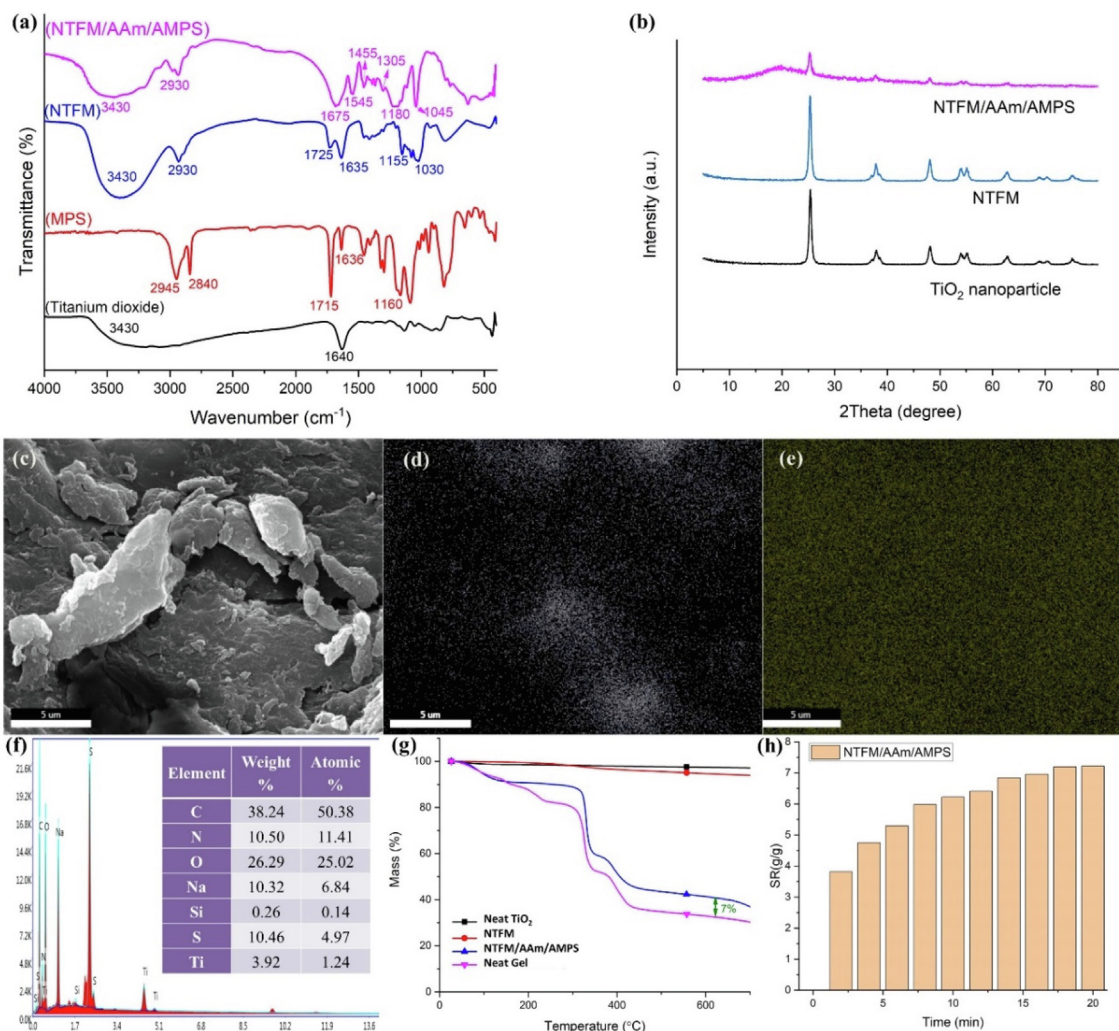
E. Rezvani Ghomi, S. Nouri Khorasani, Mohammad Sadegh Koochaki et al.

Journal of Advanced Research 43 (2023) 137–146

Fig. 2. (a) FTIR spectra and (b) XRD diffractograms of the samples. (c) FESEM micrograph of TiO$_2$ NC and distribution map of, (d) Ti element, (e) S element. (f) EDS results for the chemical composition of NTFM/AAm/AMPS. (g) TGA thermograms of neat TiO$_2$, NTFM, Neat gel, and NTFM/AAm/AMPS. (h) The SR of NTFM/AAm/AMPS.

enveloping effect of the gel at the NTFM surface [31]. From Fig. 2c, it can be seen that TiO$_2$ nanoparticles have been well-dispersed in the NC (Fig. 2d). Moreover, element S and its distribution map, Fig. 2e, attributed to AMPS monomer, shows a good dispersion of the copolymer in the NC. The formation of NTFM/AAm/AMPS NC was also confirmed with both map distributions and the EDS results of the NC chemical composition shown in Fig. 2f. The thermal stability of the neat TiO$_2$ nanoparticles, NTFM, neat gel, and NC was evaluated by a series of TGA tests. Fig. 2g presents the TGA curves for TiO$_2$ nanoparticles (Neat TiO$_2$), NTFM, AAm/AMPS gel (Neat gel), and NTFM/AAm/AMPS NC. It can be observed, from the curves, that the TiO$_2$ nanoparticles were comparatively thermally stable and were marginally decomposed. This slight weight reduction is attributed to the vaporization of physically adsorbed water on TiO$_2$ nanoparticles surfaces in the temperature range of 100 °C to 160 °C [27,36]. TGA curves of NTFM show a slight weight loss from 340 °C to 420 °C, possibly attributed to the condensation of –OH groups at the surface of nanoparticles or –OH groups in the MPS silanol groups, leading to the formation of water, which evolved at high temperature. It can be calculated from equation (1) that the E$_g$ of NTFM was approximately 1.7 wt%. TGA curves of neat gel and TiO$_2$ NCs indicate that the water loss of NTFM/AAm/AMPS below 250 °C increased with the incorporation of AAm/AMPS due to the strong hydrophilicity of AAm/AMPS networks. The thermal decomposition of NC and ammonia happened

from 250 to 450 °C. Moreover, the TiO$_2$ content was calculated at 600 °C to be 7 wt% as shown in Fig. 2. The weight loss above this temperature can be referred to as the endothermal phenomenon that occurred from the transformation of anatase TiO$_2$ into rutile TiO$_2$ [43]. The determined percentage of TiO$_2$ nanoparticles was used for the control samples in the physical and mechanical evaluation as well as the corrosion tests. The swelling performance of the NTFM/AAm/AMPS was assessed in order to investigate the absorbing ability of the NC. The NC is hydrophilic due to the existence of different polar functional groups in its chemical structure. The SR results are shown in Fig. 2h and based on that, it can be interpreted that the NC is able to absorb water up to almost 7 times its dry weight. This significant ability of the NC makes it a desirable candidate to be incorporated in the epoxy coating to absorb the corrosive media and prevent it from reaching the substrate [44].

Evaluation of coating performance

The obtained results of the Gloss tests were reported in Table 2. Although the gloss of T and NTFM samples increased with further incorporation of nanoparticles, the differences in the values were not significant and it can be claimed that the samples were all shiny [45]. The gloss of the coatings containing TiO$_2$ NC increased firstly up to 1 wt% and then decreased. The drop in the gloss of the

coatings containing 2 and 4 wt% NCs is ascribed to the roughness increment with the increase of the TiO$_2$ NC content [46].

According to the adhesion strength results presented in Table 2, incorporating neat TiO$_2$ nanoparticles decreased the adhesion strength of the coatings [47,48]. Functionalizing of TiO$_2$ nanoparticles by MPS led to a marginal decrement in the coating adhesion. The decrease in the adhesion strength of all samples can be attributed to the less integrity in the coatings. However, the decrement of the coatings' adhesion containing NTFM was lower than the T and NC samples. The better adhesion of the NTFM samples stems from the formation of the Si-O-metal covalent bonds [49]. Generally, the existence of silane coupling agents in the structure of the coating results in higher adhesion to the substrate [50]. Moreover, the incorporation of the NTFM/AAm/AMPS NC into epoxy resin decreased the adhesion of the epoxy resin, which can be attributed to a lower contact area of the resin with the substrate [51].

In general, the total elongation of the coatings relates to both adhesion and the nature of the coatings. From Table 2, it can be deduced that the introduction of modified and unmodified TiO$_2$ nanoparticles to epoxy resin decreased the adhesion of all the samples in comparison to neat epoxy coating, and hence, decreased the total elongation. This is due to the deteriorated integrity of the epoxy matrix as a result of the incorporation of external particles [45].

Assessment of self-healing performance

The EIS measurements were conducted to evaluate the anticorrosion properties of the coatings containing modified and unmodified TiO$_2$ with respect to the control sample [52,53]. Prior to the electrochemical assessment, the samples were scratched and then soaked with a 3.5 wt% NaCl aqueous solution for 18 days to reach a stable open circuit potential. Fig. 3 a. & b. show the Nyquist and Bode modulus curves of the coatings containing neat TiO$_2$ and NTFM, respectively. It should be noted that the diameter of the semicircles in Nyquist plots is regarded as the polarization resistance. Thus, the wider diameter of a sample can be considered as better anti-corrosion performance [27].

The agglomeration of TiO$_2$ nanoparticles in the C-T4 sample considerably deteriorated the corrosion resistance of the coating by increasing the matrix porosity and consequently the electrolyte diffusing through them. It can be discerned that the TiO$_2$ nanoparticle modification led to samples with less susceptibility to corrosion phenomena via corrosive media. This difference is due to the fact that C-T1, C-T2, and C-T4 samples have not been modified and the high surface energy of nanoparticles caused their agglomeration in the epoxy coating. Hence, the incorporation of neat TiO$_2$

Table 2
Physical and mechanical properties of the prepared coatings.

| Samples	Gloss (20○) (GU)	Adhesion strength (MPa)	Total elongation (%)
CTRL	87.27 ± 4.48	3.74 ± 0.03	44.82 ± 0.32
C-T1	84.07 ± 11.59	3.32 ± 0.01	36.8 ± 0.63
C-T2	89.36 ± 9.96	2.79 ± 0.03	36.8 ± 0.66
C-T4	102.07 ± 2.18	1.55 ± 0.04	13.8 ± 0.23
C-NTFM1	94.07 ± 1.11	3.14 ± 0.03	36.8 ± 0.54
C-NTFM2	87.36 ± 8.92	3.34 ± 0.03	36.8 ± 0.19
C-NTFM4	99.70 ± 6.95	3.41 ± 0.06	9.29 ± 0.64
C- NTFM/AAm/ AMPS1	97.33 ± 5.05	1.60 ± 0.01	Less than 3.01
C-NTFM/AAm/ AMPS2	88.60 ± 3.04	1.72 ± 0.04	Less than 3.01
C-NTFM/AAm/ AMPS4	59.00 ± 12.04	1.67 ± 0.05	Less than 3.01
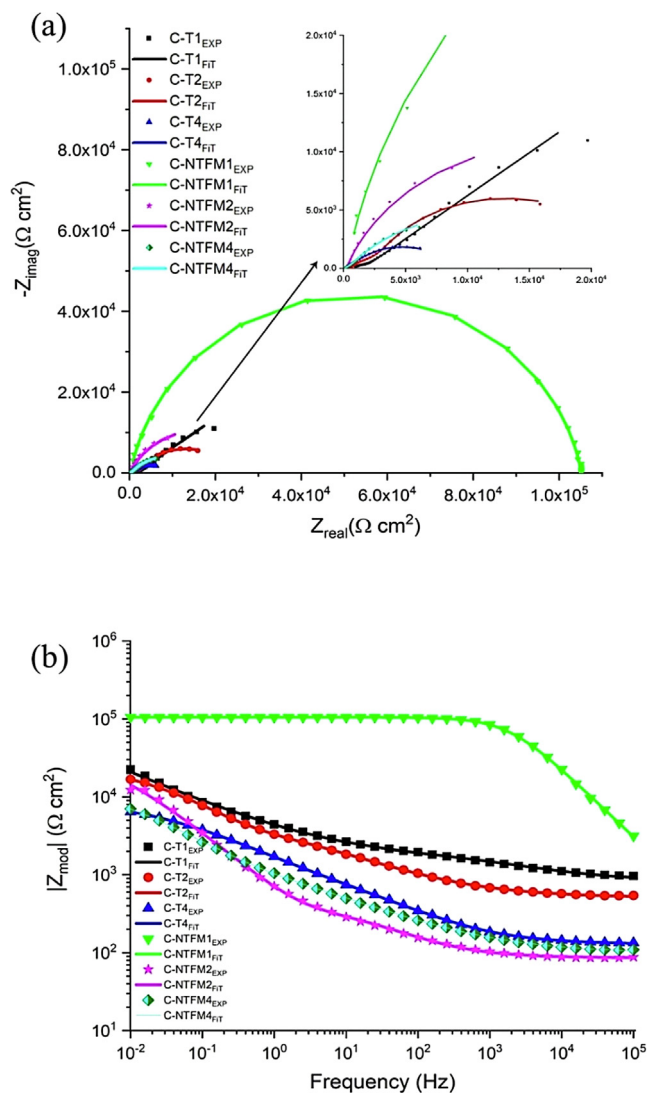
Fig. 3. (a) Nyquist & (b) Bode modulus plots of the scratched epoxy coatings containing modified and unmodified TiO$_2$ nanoparticles after immersion for 18 days in a 3.5 wt% NaCl aqueous solution.

nanoparticles enhanced the uniformity of the coatings, leading to further corrosion processes [54].

The bode modulus results of the C-T and C-NTFM samples confirmed the results of the Nyquist plots. According to Fig. 4b., the C-NTFM1 sample showed the highest impedance modulus among C-T and C-NTFM samples. It can be concluded that the incorporation of an efficient amount of nanoparticles enhanced the corrosion resistance, while the functionalization of nano-TiO$_2$ with MPS led to better dispersion and subsequently better anti-corrosion performance of the samples.

Similarly, Fig. 4 a. & b. show the Nyquist and Bode modulus curves of the coatings containing TiO$_2$ NC, respectively. In order to create a self-healing feature in the epoxy coatings, grafted AAm/AMPS copolymer gel on the NTFM samples were incorporated into them at 1, 2, and 4 wt%. According to Fig. 4a, C-NTFM/AAm/AMPS1 showed the highest corrosion resistance compared to the other samples as it had the largest Nyquist semicircle. Many inorganic nanoparticles, including TiO$_2$, have been used as corrosion inhibitors. This kind of corrosion inhibitor does not have to break to release any polymerizable healing agents, and thus their size is smaller than those containing them. In addition, their smaller size helps with their better dispersion in thin epoxy coatings
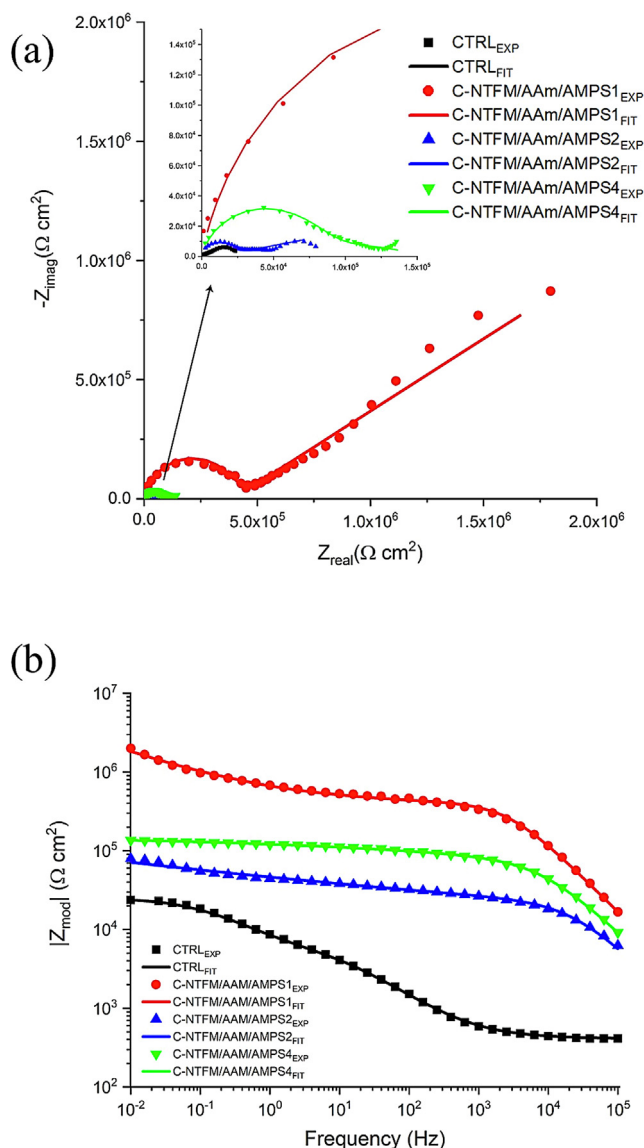
E. Rezvani Ghomi, S. Nouri Khorasani, Mohammad Sadegh Koochaki et al.

Journal of Advanced Research 43 (2023) 137–146

Fig. 4. (a) Nyquist & (b) Bode modulus plots of the scratched epoxy coatings including control and NTFM/AAm/AMPS containing samples after immersion for 18 days in a 3.5 wt% NaCl aqueous solution.

[55,56]. The existence of the TiO$_2$ nanoparticles in the structure of the NC not only promotes the segmental motion of the synthesized product but also helps to gain higher mechanical properties. Due to the AAm/AMPS gel's ability to absorb H$_2$O and the corrosive ions, if defects and cracks appear on the coatings, the NC could fill the defects and the cracks would autonomously heal, akin to intrinsic welding. This would prevent the corrosive media to reach the underlying substrate [57]. This process, also known as the defect healing mechanism, can clearly justify the self-healing mechanism of the TiO$_2$ NC when exposed to humidity and salt [34,58-60]. Comparing the Nyquist plot results of the epoxy coating containing TiO$_2$ NC with other mechanisms, such as the release of healing agents, the higher anti-corrosion property of this method is revealed [13].

Similar to Nyquist plots, the bode modulus plots confirmed the superior corrosion resistance of C-NTFM/AAm/AMPS1 among all the samples due to its higher impedance modulus in the frequency of 10^{-2} Hz. The higher impedance modulus points out the ability of the sample to protect the substrate against corrosive media [44].

From Fig. 4b, it can be discerned that the embedment of the TiO$_2$ NC into the epoxy resin noticeably raised its corrosion resistance after artificial damages and confirmed the self-healing feature of the coatings.

Fig. 5 illustrates the electrical equivalent circuit (EEC) used to obtain the EIS parameters. In this figure, R$_s$, R$_{coat}$, R$_{ct}$, CPE$_{coat}$, and CPE$_{dl}$ are the electrolyte resistance, coating resistance, charge transfer resistance, coating capacitance, and double layer capacitance, respectively. The element CPE signifies the capacitor, and n shows the potential factor in the range of −1 to 1. The ideal capacitance holds n = 1, however, normally there is a deviation in real-world scenarios [61].

All of the EIS parameters measured are shown in Table 3. Among the calculated parameters, the charge transfer resistance (R$_{ct}$) was used for quantitative analysis of the self-healing process because it is associated with the rate of Faradic processes occurring at the interface of the electrode (steel substrate). The exposed/active region of the electrode and the R$_{ct}$ have an inverse relationship. High R$_{ct}$ can be a consequence of a reduced region under the metal subjected to corrosive electrolytes [44,62]. Hence in the present research, since the exposed area of the substrate was going to be covered by the healing reactions, the higher R$_{ct}$ was correlated as higher healing efficiency [63].

Regarding the impedance parameters shown in Table 3, the modification process on the C-T1, C-T2, and C-T4 samples caused a significant improvement in corrosion resistance for sample NTFM1 in comparison with the unmodified sample C-T1. In general, a higher value of R$_{ct}$ indicates better corrosion resistance. Therefore, the NTFM1 sample was more protective than C-T1 in the corrosive media and the most corrosion-resistant sample among C-T and C-NTFM samples.

According to the EEC model and Nyquist plots, the high-frequency loop shown at the left side of the Nyquist plots indicates the dielectric behavior of the coating and the low-frequency loop at the right side of the Nyquist plots confirms the charge transfer resistance. Considering Table 3, it can be observed that for C-NTFM/AAm/AMPS samples, the value of CPE$_{coat}$ noticeably decreased, which can be ascribed to the decrement of ability in accomplishing the electrochemical reactions. From Table 3, it can be seen that the value of R$_{coat}$ for C-NTFM/AAm/AMPS2 and C-NTFM/AAm/AMPS4 are similar to each other, while C-NTFM/AAm/AMPS1 showed the best results. In addition, R$_{ct}$ was considerably raised to 2.52 × 10^{10} for C-NTFM/AAm/AMPS1 and its CPE$_{dl}$ exceptionally decreased to 1.77 × 10^{-6}, which could be a result of its efficient self-healing reactions. Furthermore, the inner surface of the C-NTFM/AAm/AMPS1 coating was significantly less than the neat epoxy coating and other C-NTFM/AAm/AMPS samples. This phenomenon can be attributed to the uniformity and homogeneity of the C-NTFM/AAm/AMPS sample. The healing efficiency (HE) of this sample was calculated to be almost 100 % by means of Eq. (3) [44,64]:
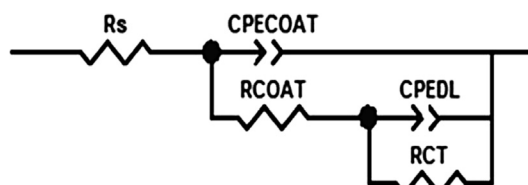
$$\%HE = (1- R_{ct0}/R_{ct}) \times 100 \qquad (3)$$

Fig. 5. Fitted electrical equivalent circuit.

E. Rezvani Ghomi, S. Nouri Khorasani, Mohammad Sadegh Koochaki et al.

Journal of Advanced Research 43 (2023) 137–146

Table 3
The EIS parameters of the scratched neat epoxy and epoxy coatings containing modified, unmodified TiO_2 nanoparticles, and TiO_2 NC.

Sample	Rs ($\Omega.cm^2$)	Rcoat ($\Omega.cm^2$)	Rct ($\Omega.cm^2$)	CPEcoat-Yo ($s^n.\Omega^{-1}.cm^{-2}$)	CPEcoat-α	CPEdl-Yo ($s^n.\Omega^{-1}.cm^{-2}$)	CPEdl-α
CTRL	4.11×10^2	6.69×10^3	1.87×10^4	1.01×10^{-5}	6.69×10^{-2}	4.97×10^{-5}	6.82×10^{-1}
C-T1	8.42×10^2	9.33×10^2	2.08×10^6	5.87×10^{-6}	5.43×10^{-1}	1.54×10^{-4}	4.08×10^{-1}
C-T2	5.09×10^2	4.48×10^3	2.15×10^4	7.78×10^{-5}	4.64×10^{-1}	1.06×10^{-4}	7.86×10^{-1}
C-T4	1.28×10^2	8.98×10^2	8.06×10^3	8.81×10^{-5}	5.68×10^{-1}	1.95×10^{-4}	4.88×10^{-1}
C-NTFM1	2.09×10^2	1.05×10^5	2.25×10^6	2.36×10^{-9}	8.87×10^{-1}	1.13×10^{-1}	7.41×10^{-1}
C-NTFM2	8.56×10^1	3.41×10^2	3.36×10^4	1.74×10^{-4}	6.24×10^{-1}	2.38×10^{-4}	8.43×10^{-1}
C-NTFM4	9.82×10^1	1.67×10^3	2.25×10^4	3.07×10^{-4}	4.39×10^{-1}	1.85×10^{-4}	7.08×10^{-1}
C-NTFM/AAm/AMPS1	1.82×10^2	3.95×10^5	2.52×10^{10}	4.93×10^{-10}	8.76×10^{-1}	1.77×10^{-6}	3.48×10^{-1}
C-NTFM/AAm/AMPS2	1.62×10^2	1.45×10^4	7.30×10^5	1.90×10^{-9}	8.48×10^{-1}	2.34×10^{-5}	1.33×10^{-1}
C-NTFM/AAm/AMPS4	5.12×10^2	2.44×10^4	1.32×10^5	1.33×10^{-9}	8.44×10^{-1}	2.15×10^{-6}	1.53×10^{-1}

Where, R_{ct0} and R_{ct} are charge transfer resistances for the neat epoxy and self-healing epoxy coatings, respectively. The obtained self-healing efficiency for NTFM/AAm/AMPS showed highly efficient results compared to other previous studies, which affirm the efficacy of using the NC mechanism [44,64].

In addition, the potentiodynamic polarization analysis was employed to assess the anti-corrosion performance of the coated samples [65]. Fig. 6a shows the chemical polarization plots for the epoxy coatings including neat TiO_2 nanoparticles and NTFM particles. Similarly, Fig. 6b represents the polarization plots for the scratched neat epoxy coating [27] and epoxy coating embedded with TiO_2 NCs at 1, 2, and 4 wt% after 18 days immersion in a 3.5 wt% NaCl solution. The plots were fitted by EC-LAB software to calculate the Tafel parameters in the potential range of $E_{OCP} \pm 0.25$ V. Furthermore, the results including corrosion potential (E_{corr}), corrosion current density (I_{corr}), and anodic/cathodic potentiodynamic polarization slopes (b_a, b_c) are presented in Table 4. The incorporation of neat TiO_2 nanoparticles in the coatings (C-T1, C-T2, and C-T4 samples) caused a lower corrosion rate of the coating when the incorporation amount was increased up to the C-T2 sample. It can be deduced from Table 4 that the modification process on the samples C-T caused a decrement in the corrosion current density. In other words, it shifted the polarization plots toward the left, as shown in Fig. 6a, which confirms that the rate of corrosion reactions diminished in the modified samples of C-NTFM1, C-NTFM2, and C-NTFM4. Thus, the surface modification of nano-TiO_2 by MPS caused their better dispersion throughout the epoxy resin and consequently prevented the agglomeration of TiO_2 nanoparticles, leading to the better corrosion resistance of C-NTFM, compared to the C-T samples. In addition, the agglomeration of TiO_2 nanoparticles in the C-T4 sample considerably deteriorated the anti-corrosion performance of the sample. Therefore, the modification of the TiO_2 nanoparticles made the samples less susceptible to corrosion via the corrosive media. Hence, the incorporation of neat TiO_2 nanoparticles increased the uniformity of the coatings, leading to further corrosion processes [54].

In order to develop corrosion resistance, grafted AAm/AMPS copolymer gel on the NTFM samples was incorporated into the epoxy resin. Due to the AAm/AMPS gel's affinity towards the water and the corrosive ions, if defects and cracks appear on the coatings, the NC would fill the defects. Therefore, the cracks autonomously heal, similar to intrinsic welding, and prevent the corrosive media from reaching the underlying substrate. This process can clearly justify the self-healing mechanism of TiO_2 NC when exposed to humidity and salt [34,59]. The coated samples were prepared in three different weight percentages at 1, 2, and 4 wt% of the NTFM/AAm/AMPS and incorporated into the epoxy matrix. According to Table 4, the I_{corr} of the C-NTFM/AAm/AMPS1 sample was lower than the others, which means that this sample exhibited the best corrosion behavior compared to other specimens [33]. Moreover, the healing efficiency (HE) for the C-NTFM/AAm/AMPS1 sample was higher than the others by an amount of 98%, calculated from Eq. (4).
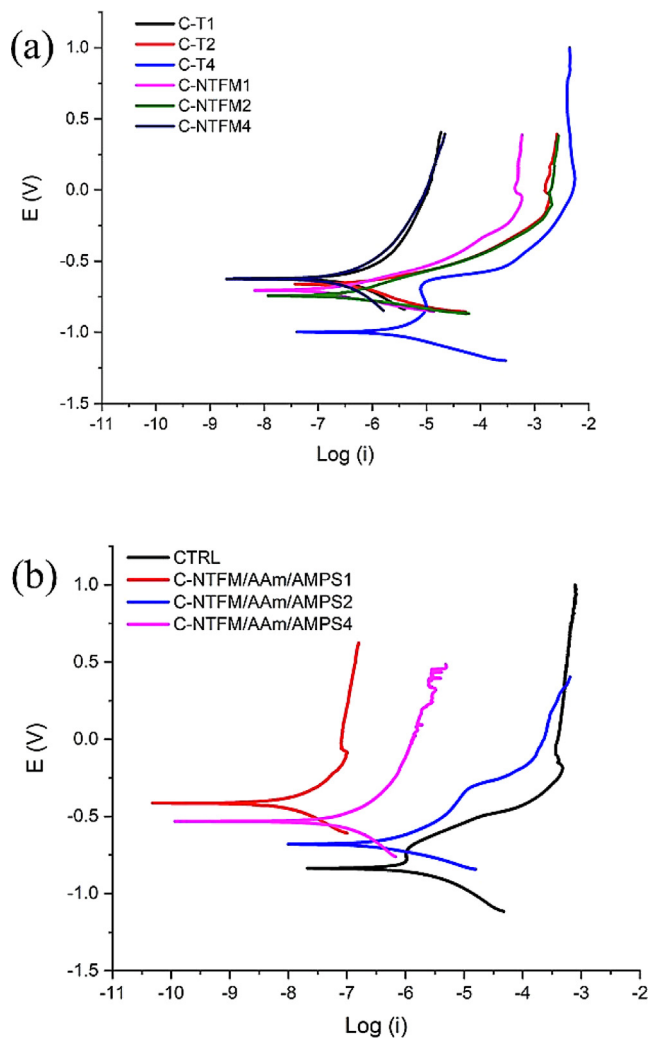

Fig. 6. The Tafel plots of the scratched coatings after immersion for 18 days in a 3.5 wt% NaCl aqueous solution: (a) the epoxy coating containing modified and unmodified TiO_2 nanoparticles, (b) neat epoxy and epoxy coatings containing TiO_2 NC.

$$\% \text{ HE} = [(I_{corr0} - I_{corr})/I_{corr0}] \times 100 \qquad (4)$$

Where, I_{corr0} and I_{corr} are the corrosion current density of neat epoxy coating and the self-healing epoxy coatings, respectively.

It should be noted that the value of E_{corr} significantly shifted to the positive direction via the surface modification of TiO_2 nanoparticles. The higher E_{corr} value shows that the potential energy for corrosion reaction increased and caused a significant reduction in the corrosion process. In the research study conducted by Atta

Table 4
The Tafel parameters of the scratched neat epoxy and epoxy coatings containing modified, unmodified TiO$_2$ nanoparticles, and TiO$_2$ NC.

Sample	I$_{corr}$ (µA)	E$_{corr}$ (mV)	b$_a$ (mV)	b$_c$ (mV)
CTRL	0.671	−751.116	288.4	204.3
C-T1	0.341	−632.351	265.1	217.6
C-T2	0.522	−702.89	113.1	99.7
C-T4	2.584	−1018.227	356.6	99.4
C-NTFM1	0.111	−730.97	108.5	62.2
C-NTFM2	0.154	−745.383	102.5	51.6
C-NTFM4	0.234	−630.546	266.5	287.6
C-NTFM/AAm/AMPS1	0.009	−435.893	310.8	190.6
C-NTFM/AAm/AMPS2	0.068	−744.754	46	25
C-NTFM/AAm/AMPS4	0.074	−530.325	305.9	264.4

et al. [44], magnetite nanoparticles were functionalized by AMPS, AAm/AMPS, and AMPS/Acrylic acid gels and were incorporated in the epoxy resin. Among the samples, AMPS/AAm magnetite NC provided the maximum HE of 91.1% and 91.3% by EIS and potentiodynamic polarization, respectively. In another study, the authors used the same self-healing mechanism as the current study and reached a maximum HE of 88% with both EIS and potentiodynamic polarization methods [64]. Comparing these studies with the current one, it can be concluded that using TiO$_2$ nanoparticles with AMPS/AAm gel was more effective to induce self-healing properties. It is noteworthy to mention that no delamination was observed between the coatings and the substrate during the immersion period. In addition, only a minor sign of corrosion products was observed in the scratched area as a result of electrolyte penetration in the scratch at the initial stages of immersion, which was then stopped due to the crack closure by the healing process. Moreover, no corrosion product was observed under the applied coatings.

Conclusions

An anti-corrosive and self-healing coating was prepared through the synthesis and the embedment of modified TiO$_2$ nanoparticles. The functionalization and grafting of particles by MPS, as the coupling agent, and AAm/AMPS NC improved the corrosion behavior of the samples. The self-healing performance of NTFM/AAm/AMPS coatings was assessed according to the corrosion properties of the scratched panels. In comparison with the neat epoxy sample, the anti-corrosion performance of the sample containing 1 wt% NTFM/AAm/AMPS was noticeably enhanced. The existence of the flexible layer on the nanoparticles' surface aided the superior dispersion of nanoparticles, their ability to absorb the corrosive components, and their swelling, which prevented the corrosive components from reaching the underlying substrate.

Human and animal rights

This article does not contain any studies with human or animal subjects.

CRediT authorship contribution statement

Erfan Rezvani Ghomi: Conceptualization, Methodology, Investigation, Data curation, Writing – original draft, Writing – review & editing, Visualization. **Saied Nouri Khorasani:** Conceptualization, Resources, Project administration, Supervision, Writing – original draft, Writing – review & editing. **Mohammad Sadegh Koochaki:** Data curation, Formal analysis, Methodology, Software, Validation, Visualization, Writing – original draft, Writing – review & editing. **Mohammad Dinari:** Resources, Writing – original draft, Writing – review & editing. **Shahla Ataei:** Conceptualization, Methodology, Validation, Writing – original draft, Writing – review & editing. **Mohammad Hossein Enayati:** Data curation, Writing – original draft, Writing – review & editing. **Oisik Das:** Data curation, Methodology, Project administration, Validation, Writing – original draft, Writing – review & editing. **Rasoul Esmaeely Neisiany:** Conceptualization, Data curation, Methodology, Resources, Software, Supervision, Validation, Writing – original draft, Writing – review & editing.

Declaration of Competing Interest

The authors declare that they have no known competing financial interests or personal relationships that could have appeared to influence the work reported in this paper.

Acknowledgments

References

[1] Eddy NO. Experimental and theoretical studies on some amino acids and their potential activity as inhibitors for the corrosion of mild steel, part 2. J Adv Res 2011;2(1):35–47.
[2] Ferri M, Trueba M, Trasatti Stefano P, Cabrini M, Conte Antonietta L. Electrochemical investigation of corrosion and repassivation of structural aluminum alloys under permanent load in bending. Corros Rev 2017;35(4–5):225–39.
[3] Ataei S, Khorasani SN, Neisiany RE. Biofriendly vegetable oil healing agents used for developing self-healing coatings: A review. Prog Org Coat 2019;129:77–95.
[4] Chang K-C, Hsu M-H, Lu H-I, Lai M-C, Liu P-J, Hsu C-H, et al. Room-temperature cured hydrophobic epoxy/graphene composites as corrosion inhibitor for cold-rolled steel. Carbon 2014;66:144–53.
[5] Gao W, Chen X, Chen D. Genetic programming approach for predicting service life of tunnel structures subject to chloride-induced corrosion. J Adv Res 2019;20:141–52.
[6] Hammi M, Ziat Y, Zarhri Z, Laghlimi C, Moutcine A. Epoxy/alumina composite coating on welded steel 316L with excellent wear and anticorrosion properties. Sci Rep 2021;11(1):12928.
[7] Dordane R, Doroodmand MM. Novel method for scalable synthesis of wollastonite nanoparticle as nano-filler in composites for promotion of anti-corrosive property. Sci Rep 2021;11(1):2579.
[8] Jagtap RN, Patil PP, Hassan SZ. Effect of zinc oxide in combating corrosion in zinc-rich primer. Prog Org Coat 2008;63(4):389–94.
[9] Khoo YS, Lau WJ, Liang YY, Karaman M, Gürsoy M, Ismail AF. Eco-friendly surface modification approach to develop thin film nanocomposite membrane with improved desalination and antifouling properties. J Adv Res 2022;36:39–49.
[10] Zhao X, Chen C, Xu W, Zhu Q, Ge C, Hou B. Evaluation of long-term corrosion durability and self-healing ability of scratched coating systems on carbon steel in a marine environment. Chin J Oceanol Limnol 2017;35(5):1094–107.
[11] Ghazizadeh A, Haddadi SA, Mahdavian M. The effect of sol–gel surface modified silver nanoparticles on the protective properties of the epoxy coating. RSC Adv 2016;6(23):18996–9006.
[12] Wahby MH, Atta AM, Al-Lohedan HA, El-Saeed AM, Tawfik AM. Non-Cracked Epoxy Nanogel Composite as Anticorrosive Coatings for Aggressive Marine Environment. Int J Electrochem Sci 2017;12:316–29.

[13] Koochaki MS, Nouri Khorasani S, Esmaeely Neisiany R, Ashrafi A, Magni M, Trasatti SP. Facile strategy toward the development of a self-healing coating by electrospray method. Mater Res Express 2019;6(11):116444. doi: https://doi.org/10.1088/2053-1591/ab4d1b.

[14] Wu X, Yang F, Gan J, Zhao W, Wu Y. A flower-like waterborne coating with self-cleaning, self-repairing properties for superhydrophobic applications. J Mater Res Technol 2021;14:1820–9.

[15] Esmaeely Neisiany R, Enayati MS, Sajkiewicz P, Pahlevanneshan Z, Ramakrishna S. Insight Into the Current Directions in Functionalized Nanocomposite Hydrogels. Front Mater 2020;7:25.

[16] Wang S, Urban MW. Self-healing polymers. Nat Rev Mater 2020;5(8):562–83.

[17] Wang Z, Scheres L, Xia H, Zuilhof H. Developments and Challenges in Self-Healing Antifouling Materials. Adv Funct Mater 2020;30(26):1908098. doi: https://doi.org/10.1002/adfm.201908098.

[18] Zhang L, Guan Q, Shen Ao, Neisiany RE, You Z, Zhu M. Supertough spontaneously self-healing polymer based on septuple dynamic bonds integrated in one chemical group. Sci. China Chem. 2022;65(2):363–72.

[19] Sanka RVSP, Krishnakumar B, Leterrier Y, Pandey S, Rana S, Michaud V. Soft Self-Healing Nanocomposites. Front Mater 2019;6:137.

[20] Zhang H, Lin B, Tang J, Wang Y, Wang H, Zhang H, et al. An ethyl cellulose-based supramolecular gel composite coating for metal corrosion protection and its self-healing property from electromagnetic heating effect. Surf Coat Technol 2021;424:127647.

[21] Habib S, Hassanein A, Kahraman R, Mahdi Ahmed E, Shakoor RA. Self-healing behavior of epoxy-based double-layer nanocomposite coatings modified with Zirconia nanoparticles. Mater Des 2021;207:109839.

[22] Keshmiri N, Najmi P, Ramezanzadeh B, Ramezanzadeh M, Bahlakeh G. Nano-scale P, Zn-codoped reduced-graphene oxide incorporated epoxy composite; synthesis, electronic-level DFT-D modeling, and anti-corrosion properties. Prog Org Coat 2021;159:106416.

[23] Cheng Li, Liu C, Wu H, Zhao H, Wang L. Interfacial assembled mesoporous polydopamine nanoparticles reduced graphene oxide for high performance of waterborne epoxy-based anticorrosive coatings. J Colloid Interface Sci 2022;606:1572–85.

[24] Ghorbani M, Ebrahimnezhad-Khaljiri H, Eslami-Farsani R, Vafaeenezhad H. The synergic effect of microcapsules and titanium nanoparticles on the self-healing and self-lubricating epoxy coatings: A dual smart application. Surf Interfaces 2021;23:100998.

[25] Pirhady Tavandashti N, Molana Almas S, Esmaeilzadeh E. Corrosion protection performance of epoxy coating containing alumina/PANI nanoparticles doped with cerium nitrate inhibitor on Al-2024 substrates. Prog Org Coat 2021;152:106133.

[26] Habib S, Fayyad E, Shakoor RA, Kahraman R, Abdullah A. Improved self-healing performance of polymeric nanocomposites reinforced with talc nanoparticles (TNPs) and urea-formaldehyde microcapsules (UFMCs). Arabian J Chem 2021;14(2):102926. doi: https://doi.org/10.1016/j.arabjc.2020.102926.

[27] Ghomi ER, Khorasani SN, Kichi MK, Dinari M, Ataei S, Enayati MH, et al. Synthesis and characterization of TiO2/acrylic acid-co-2-acrylamido-2-methyl propane sulfonic acid nanogel composite and investigation its self-healing performance in the epoxy coatings. Colloid Polym Sci 2020;298(2):213–23.

[28] Fadl AM, Abdou MI, Hamza MA, Sadeek SA. Corrosion-inhibiting, self-healing, mechanical-resistant, chemically and UV stable PDMAS/TiO2 epoxy hybrid nanocomposite coating for steel petroleum tanker trucks. Prog Org Coat 2020;146:105715.

[29] Habib S, Fayyad E, Nawaz M, Khan A, Shakoor RA, Kahraman R, et al. Cerium Dioxide Nanoparticles as Smart Carriers for Self-Healing Coatings. Nanomaterials 2020;10(4):791. doi: https://doi.org/10.3390/nano10040791.

[30] Atta AM, Ezzat AO, El-Saeed AM, Tawfeek AM, Sabeela NI. Self-healing of chemically bonded hybrid silica/epoxy for steel coating. Prog Org Coat 2020;141:105549.

[31] El-Mahdy G, Atta A, Al-Lohedan H, Tawfeek A, Abdel-Khalek AA. Synthesis of Encapsulated Titanium Oxide Sodium 2-Acrylamido-2-methylpropan Sulfonate Nanocomposite for Preventing the Corrosion of steel. Int J Electrochem Sci 2015;10:5702–13.

[32] Sheng X, Xie D, Wang C, Zhang X, Zhong Li. Synthesis and characterization of core/shell titanium dioxide nanoparticle/polyacrylate nanocomposite colloidal microspheres. Colloid Polym Sci 2016;294(2):463–9.

[33] Rezvani Ghomi E, Esmaeely Neisiany R, Nouri Khorasani S, Dinari M, Ataei S, Koochaki MS, et al. Development of an epoxy self-healing coating through the incorporation of acrylic acid-co-acrylamide copolymeric gel. Prog Org Coat 2020;149:105948.

[34] Atta AM, Al-Lohedan HA, El-saeed AM, Al-Shafey HI, Wahby MH. Epoxy embedded with TiO2 nanogel composites as promising self-healing organic coatings of steel. Prog Org Coat 2017;105:291–302.

[35] Atta AM, El-Saeed AM, Al-Lohedan HA, Wahby M. Effect of Montmorillonite Nanogel Composite Fillers on the Protection Performance of Epoxy Coatings on Steel Pipelines. Molecules 2017;22(6):905.

[36] Zhao J, Milanova M, Warmoeskerken MMCG, Dutschk V. Surface modification of TiO2 nanoparticles with silane coupling agents. Colloids Surf, A 2012;413:273–9.

[37] Jamshidi H, Rabiee A. Synthesis and Characterization of Acrylamide-Based Anionic Copolymer and Investigation of Solution Properties. Adv Mater Sci Eng 2014;2014:6.

[38] Xin H, Ao D, Wang X, Zhu Y, Zhang J, Tan Y. Synthesis, characterization, and properties of copolymers of acrylamide with sodium 2-acrylamido-2-methylpropane sulfonate with nano silica structure. Colloid Polym Sci 2015;293(5):1307–16.

[39] Rosa F, Bordado J, Casquilho M. Kinetics of water absorbency in AA/AMPS copolymers: applications of a diffusion–relaxation model. Polymer 2002;43(1):63–70.

[40] Koochaki MS, Khorasani SN, Neisiany RE, Ashrafi A, Trasatti SP, Magni M. A highly responsive healing agent for the autonomous repair of anti-corrosion coatings on wet surfaces. In operando assessment of the self-healing process. J Mater Sci 2021;56(2):1794–813.

[41] El Mahdy GA, Atta AM, Dyab AKF, Al-Lohedan HA. Protection of Petroleum Pipeline Carbon Steel Alloys with New Modified Core-Shell Magnetite Nanogel against Corrosion in Acidic Medium. J Chem 2013;2013:9.

[42] Mahire VN, Patel VE, Chaudhari AB, Gite VV, Mahulikar PP. Silane@TiO2nanoparticles-driven expeditious synthesis of biologically active benzo[4,5]imidazo[1,2-a]chromeno[4,3-d]pyrimidin-6-one scaffolds: A green approach. J Chem Sci 2016;128(4):671–9.

[43] Wang X, Hu D, Yang J. Synthesis of PAM/TiO2 Composite Microspheres with Hierarchical Surface Morphologies. Chem Mater 2007;19(10):2610–21.

[44] Atta AM, El-Azabawy OE, Ismail HS, Hegazy MA. Novel dispersed magnetite core–shell nanogel polymers as corrosion inhibitors for carbon steel in acidic medium. Corros Sci 2011;53(5):1680–9.

[45] Işın D, Kayaman-Apohan N, Güngör A. Preparation and characterization of UV-curable epoxy/silica nanocomposite coatings. Prog Org Coat 2009;65(4):477–83.

[46] Ataei S, Khorasani SN, Torkaman R, Neisiany RE, Koochaki MS. Self-healing performance of an epoxy coating containing microencapsulated alkyd resin based on coconut oil. Prog Org Coat 2018;120:160–6.

[47] Sørensen PA, Kiil S, Dam-Johansen K, Weinell CE. Anticorrosive coatings: a review. Journal of Coatings Technology Research 2009;6(2):135–76.

[48] Pourhashem S, Rashidi A, Vaezi MR, Bagherzadeh MR. Excellent corrosion protection performance of epoxy composite coatings filled with amino-silane functionalized graphene oxide. Surf Coat Technol 2017;317:1–9.

[49] Lamaka SV, Xue HB, Meis NNAH, Esteves ACC, Ferreira MGS. Fault-tolerant hybrid epoxy-silane coating for corrosion protection of magnesium alloy AZ31. Prog Org Coat 2015;80:98–105.

[50] Plueddemann EP. Silane adhesion promoters in coatings. Prog Org Coat 1983;11(3):297–308.

[51] Tatiya PD, Hedaoo RK, Mahulikar PP, Gite VV. Novel Polyurea Microcapsules Using Dendritic Functional Monomer: Synthesis, Characterization, and Its Use in Self-healing and Anticorrosive Polyurethane Coatings. Ind Eng Chem Res 2013;52(4):1562–70.

[52] Eddy NO, Momoh-Yahaya H, Oguzie EE. Theoretical and experimental studies on the corrosion inhibition potentials of some purines for aluminum in 0.1M HCl. J Adv Res 2015;6(2):203–17.

[53] Farzi G, Davoodi A, Ahmadi A, Neisiany RE, Anwer MK, Aboudzadeh MA. Encapsulation of Cerium Nitrate within Poly(urea-formaldehyde) Microcapsules for the Development of Self-Healing Epoxy-Based Coating. ACS Omega 2021;6(46):31147–53.

[54] Shi H, Liu F, Yang L, Han E. Characterization of protective performance of epoxy reinforced with nanometer-sized TiO2 and SiO2. Prog Org Coat 2008;62(4):359–68.

[55] Zhang F, Ju P, Pan M, Zhang D, Huang Y, Li G, et al. Self-healing mechanisms in smart protective coatings: A review. Corros Sci 2018;144:74–88.

[56] Wang L, Wang L, Wu J, Wang L, Cong W, Wang X, et al. Exploring the mechanism of self-stratifying coatings with aggregation-induced emission. Prog Org Coat 2021;159:106448.

[57] Thakur VK, Kessler MR. Self-healing polymer nanocomposite materials: A review. Polymer 2015;69:369–83.

[58] Atta AM, Al-Lohedan HA, El-Saeed AM, Al-Shafey HI, Wahby M. Salt-controlled self-healing nanogel composite embedded with epoxy as environmentally friendly organic coating. J Coat Technol Res 2017;14(5):1225–36.

[59] Yu Z, Di H, Ma Yu, He Yi, Liang L, Lv L, et al. Preparation of graphene oxide modified by titanium dioxide to enhance the anti-corrosion performance of epoxy coatings. Surf Coat Technol 2015;276:471–8.

[60] Hughes AE, Cole IS, Muster TH, Varley RJ. Designing green, self-healing coatings for metal protection. NPG Asia Mater 2010;2(4):143–51.

[61] Yeganeh M, Asadi N, Omidi M, Mahdavian M. An investigation on the corrosion behavior of the epoxy coating embedded with mesoporous silica nanocontainer loaded by sulfamethazine inhibitor. Prog Org Coat 2019;128:75–81.

[62] Wang W, Xu L, Li X, Lin Z, Yang Yi, An E. Self-healing mechanisms of water triggered smart coating in seawater. J Mater Chem A 2014;2(6):1914–21.

[63] Koochaki MS, Neisiany RE, Khorasani SN, Ashrafi A, Trasatti SP, Magni M. The influence of the healing agent characteristics on the healing performance of epoxy coatings: Assessment of the repair process by EIS technique. Prog Org Coat 2021;159:106431.

[64] Atta A, El-Mahdy G, Al-Lohedan H, Al-Hussain S. Synthesis of Environmentally Friendly Highly Dispersed Magnetite Nanoparticles Based on Rosin Cationic Surfactants as Thin Film Coatings of Steel. Int J Mol Sci 2014;15(4):6974–89.

[65] Muthirulan P, Kannan N, Meenakshisundaram M. Synthesis and corrosion protection properties of poly(o-phenylenediamine) nanofibers. J Adv Res 2013;4(4):385–92.